

Implications from GW170817 and I-Love-Q relations for relativistic hybrid stars

Vasileios Paschalidis,¹ Kent Yagi,² David Alvarez-Castillo,^{3,4} David B. Blaschke,^{3,5,6} and Armen Sedrakian⁷

¹*Theoretical Astrophysics Program, Departments of Astronomy and Physics,
University of Arizona, 933 N. Cherry Ave., Tucson, AZ 85721*

²*Department of Physics, University of Virginia, Charlottesville, Virginia 22904, USA*

³*Bogoliubov Laboratory of Theoretical Physics, Joint Institute for Nuclear Research, 141980 Dubna, Russia*

⁴*ExtreMe Matter Institute EMMI, GSI Helmholtzzentrum für
Schwerionenforschung, Planckstraße 1, 64291 Darmstadt, Germany*

⁵*Institute of Theoretical Physics, University of Wrocław, 50-204 Wrocław, Poland*

⁶*National Research Nuclear University (MEPhI), 115409 Moscow, Russia*

⁷*Frankfurt Institute for Advanced Studies, D-60438 Frankfurt-Main, Germany*

(Dated: May 7, 2018)

Gravitational wave observations of GW170817 placed bounds on the tidal deformabilities of compact stars allowing one to probe equations of state for matter at supranuclear densities. Here we design new parametrizations for hybrid hadron-quark equations of state, that give rise to low-mass twin stars, and test them against GW170817. We find that GW170817 is consistent with the coalescence of a binary hybrid star–neutron star. We also test and find that the I-Love-Q relations for hybrid stars in the third family agree with those for purely hadronic and quark stars within $\sim 3\%$ for both slowly and rapidly rotating configurations, implying that these relations can be used to perform equation-of-state independent tests of general relativity and to break degeneracies in gravitational waveforms for hybrid stars in the third family as well.

I. INTRODUCTION

The direct detection of gravitational waves (GWs) by the LIGO and Virgo Scientific Collaborations (LVC) has already started to revolutionize our understanding of the cosmos. The LVC direct detections of GWs, consistent with the inspiral and merger of binary black holes [1–5], solidified the onset of the era of GW astronomy, and provided a number of astrophysics and fundamental physics implications (see, e.g., [3, 6–8]). The recent simultaneous detection of a GW signal by the LVC [9] (event GW170817) and a gamma-ray burst (GRB) by the Fermi satellite [10], including subsequent counterpart electromagnetic signals [11–18], have ushered us in the era of “multimessenger” astronomy, astrophysics and cosmology [19].

The impact of GW170817 on astrophysics [20] and fundamental physics is far reaching. For example, GW170817 and GRB 170817A provided the best evidence, yet, that some GRBs are associated with the merger of binary compact stars as envisioned by [21–23] and recently demonstrated numerically in [24, 25] (see also [26, 27] for recent reviews). GW170817 placed constraints on the properties of the progenitor of the binary compact object GW170817 [28], and the GW background from compact binaries [29]. Moreover, GW170817 and GRB 170817A constrained the speed of gravity, the equivalence principle and Lorentz invariance [10], consequently constraining to a large degree gravity theories designed to explain the accelerated expansion of the Universe without dark energy [30–37] (see also [38, 39] for earlier work). Furthermore, GW170817 furnished the first ever “standard siren” [40] measurement of the Hubble constant [19].

Another important impact of GW170817 on funda-

mental physics is that GW170817 set bounds on the tidal deformabilities (TDs) of compact stars [9]. The observation of $2M_{\odot}$ pulsars [41–44] had already set a tight constraint on the properties of nuclear matter, requiring its equation of state (EOS) to be stiff, see, e.g., [45–47]. However, GW170817 has “raised the bar” compact star EOSs must pass to be physically viable: *candidate EOSs must now also satisfy the GW170817 constraints on the TD of compact stars.*

A study of the consequences of the GW170817 TD bounds on the nuclear EOS was performed in [48]. Multimessenger observations of GW170817 were also used to place constraints on nonspinning neutron star (NS) masses and radii using approaches with a varying number of assumptions, see, e.g., [49–55]. However, these previous works did not consider EOSs that support a strong phase transition with a sufficiently large jump in energy density to give rise to a separate (third family) branch of compact stars like the EOSs we develop here.

In this work, we investigate how GW170817 can constrain the properties of *hybrid compact stars* which have a strong hadron-quark phase transition in their interiors. In particular, we mainly focus on EOSs allowing a *third family* of stable compact objects at low mass, i.e., in addition to the stable branches of white dwarfs and NSs. The third family of compact stars, which has been studied over several decades [56–59]), arises when there is an instability region separating hadronic NSs from hybrid stars (HSs); this leads to the emergence of twins - NSs and HSs having the same mass but different radii [59]. The HS internal structure requires a single-phase quark core enclosed by a hadronic shell with a first-order phase transition at their interface. An additional phase transition in the quark core can lead to a fourth family of compact stars [47], but we do not consider this possibil-

ity here.

In this paper we develop *new parametrizations* of hybrid hadron-quark EOSs that allow for a third family of compact stars to emerge at “low mass” ($\sim 1.5M_\odot$) and are consistent with the existence of $2M_\odot$ pulsars. We investigate whether these EOSs are consistent with GW170817 by computing the TD of corresponding compact stars. Moreover, we compute the I-Love-Q relations [60, 61] (see also [62–64] for recent reviews) for slowly and rapidly rotating HSs in the third family constructed with these EOSs and compare them to the I-Love-Q relations of purely hadronic and quark stars. It is important to test the universality of I-Love-Q relations because HSs in the third family have a sharp first-order phase transition at the hadron-quark interface in their interior, and it is not a priori clear that such HSs satisfy the neutron and quark star I-Love-Q relations [65]. Once established also for 3rd family and hybrid stars, the I-Love-Q relations can be used to perform equation-of-state independent tests of general relativity and to break degeneracies in GWs [60, 61]. Thus, it is important to know if these relations hold for HSs in the third family. Throughout, we adopt geometrized units unless otherwise stated.

II. EQUATIONS OF STATE

The new parametrizations of EOSs we develop here describe zero-temperature nuclear matter in β -equilibrium with a low-density phase of nucleonic matter and high-density phase of quark matter. We consider two sets of EOSs which cover a range of current models as described in [47] (Set-I) and [46] (Set-II).

In Set I the low-density phase is based on a covariant density functional theory [66] with density-dependent couplings [67], as applied to hadronic matter in [68]. The Lagrangian underlying the density functional, and the corresponding zero-temperature pressure of nucleonic matter are given in Eqs. (1) and (2) in [68], respectively.

Our Set II consists of EOSs labeled ACB4-7. The low-density regime ($n \leq n_0$) of these EOSs is equivalent to Set I. Above the saturation density $n_0 = 0.16 \text{ fm}^{-3}$, but below the deconfinement phase transition, EOSs ACB4 and ACB5 correspond to the stiffest EOS of [69], while the EOSs ACB6 and ACB7 fit the density-dependent relativistic mean field EOS DD2-p30 [70] accounting for nucleonic excluded volume effects in that region.

In general, there exist two prescriptions for matching the low-density nucleonic EOS to the quark matter EOS; which one is realized in nature depends on the surface tension between nuclear and quark matter [71, 72]. If the tension between these phases is low, a mixed phase of quark and nucleonic matter is formed in-between purely nuclear and quark matter phases. Conversely, if the tension is high, a sharp transition boundary is energetically favorable. In the latter case, there is a jump in the energy density at a certain transition pressure at which the

baryochemical potentials of both phases coincide. Since the surface tension is presently not known accurately, both prescriptions are viable. Here we consider the second case assuming that the surface tension between the quark matter and nucleonic phases is high enough to sustain a sharp boundary between them. In all our models the pressure matching between the phases is performed via a standard Maxwell construction.

For the Set I quark matter EOS, we use the constant speed of sound parametrization [73], see also [47, 74, 75]. The pressure beyond the point where the phase transitions to quark matter takes place is given analytically by

$$P(\varepsilon) = \begin{cases} P_{\text{tr}}, & \varepsilon_1 \leq \varepsilon \leq \varepsilon_2, \\ P_{\text{tr}} + c_s^2(\varepsilon - \varepsilon_2), & \varepsilon > \varepsilon_2, \end{cases} \quad (1)$$

where $P_{\text{tr}} = P(\varepsilon_1) = P(\varepsilon_2)$ is the value of the (transition) pressure in the energy density range $\varepsilon_1 \leq \varepsilon \leq \varepsilon_2$, and c_s is the sound speed of the quark matter phase. It is convenient to parametrize the magnitude of the jump via a parameter j , as $\Delta\varepsilon \equiv \varepsilon_2 - \varepsilon_1 = \varepsilon_1 j$. Within Set I we consider two subsets that we call “ACS-I” and “ACS-II”. The values of the parameters for these EOSs are presented in Table I.

The ACS-I models, as we shall see below, generate high mass $M/M_\odot \simeq 2$ twins, as well as twins when $j = 0.6$. The ACS-II models produce low-mass $M/M_\odot \simeq 1.5$ HSs as well as twins for $j = 0.8$ and 1.0 . In the ACS-II models, the choice of maximally stiff quark matter EOS allows for massive $\sim 2M_\odot$ compact stars. EOSs with these properties have been obtained recently within a relativistic density functional approach to quark matter [76–78].

TABLE I. Parameters for the ACS-I and ACS-II EOS models that adopt constant speed of sound parametrization. The parameters have the same meaning as in Eq. (1) in the main text, and j parametrizes the phase transition energy density jump as $\Delta\varepsilon \equiv \varepsilon_1 j$. The last column gives the maximum masses M_{max} .

ACS	j	P_{tr}	ε_1/c^2	$(c_s/c)^2$	M_{max}
		[$10^{34} \text{ dyn cm}^{-2}$]	[$10^{14} \text{ g cm}^{-3}$]		[M_\odot]
I	0.10	17.0	8.34	0.8	2.47
	0.27	17.0	8.34	0.8	2.31
	0.43	17.0	8.34	0.8	2.17
	0.60	17.0	8.34	0.8	2.05
II	0.80	8.34	6.58	1.0	2.08
	1.00	8.34	6.58	1.0	1.97

For the Set II (labeled “ACB”) we employ a piecewise polytropic representation [69, 79, 80] of the EOS at supersaturation densities ($n_1 < n < n_5 \gg n_0$)

$$P(n) = \kappa_i (n/n_0)^{\Gamma_i}, \quad n_i < n < n_{i+1}, \quad i = 1 \dots 4, \quad (2)$$

where Γ_i is the polytropic index in one of the density regions labeled by $i = 1 \dots 4$. The first polytrope describes a stiff nucleonic EOS. The second polytrope corresponds to a first-order phase transition with a constant pressure

$P_{tr} = \kappa_2 (\Gamma_2 = 0)$. The polytropes in regions 3 and 4 above the phase transition correspond to high-density matter, e.g., stiff quark matter.

TABLE II. EOS models ACB4-ACB7. The parameters have the same meaning as in Eq. (2) in the main text. The first polytrope ($i = 1$) parametrizes the nuclear EOS at supersaturation densities, the second polytrope ($i = 2$) corresponds to a first-order phase transition with a constant pressure P_{tr} for densities between n_2 and n_3 . The polytropes in regions 3 and 4 above the phase transition correspond to high-density matter, e.g., quark matter. The last column gives the maximum masses M_{\max} on the hadronic (hybrid) branch corresponding to region 1 (4). The minimal mass M_{\min} on the hybrid branch is given for region 3.

ACB	i	Γ_i	κ_i [MeV/fm ³]	n_i [1/fm ³]	$m_{0,i}$ [MeV]	$M_{\max/\min}$ [M_{\odot}]
4	1	4.921	2.1680	0.1650	939.56	2.01
	2	0.0	63.178	0.3174	939.56	–
	3	4.000	0.5075	0.5344	1031.2	1.96
	4	2.800	3.2401	0.7500	958.55	2.11
5	1	4.777	2.1986	0.1650	939.56	1.40
	2	0.0	33.969	0.2838	939.56	–
	3	4.000	0.4373	0.4750	995.03	1.39
	4	2.800	2.7919	0.7500	932.48	2.00
6	1	4.2602	2.3096	0.1650	939.56	2.00
	2	0.0	78.329	0.3659	939.56	–
	3	4.000	0.3472	0.6201	1050.3	1.93
	4	2.800	2.7589	0.9000	964.49	2.00
7	1	4.408	2.2773	0.1650	939.56	1.50
	2	0.0	41.316	0.3088	939.56	–
	3	4.000	0.4124	0.5062	1003.20	1.49
	4	2.800	4.9726	0.8300	883.29	2.00

The Set II EOS parameters are given in Table II. Note that ACB5 (ACB7) requires that the phase transition onset occurs at a nucleon number density of 0.284 (0.309) fm⁻³, i.e., at roughly two times the nuclear saturation density. While this density seems to be on the low end, we recall that in our case we have asymmetric nuclear matter, so that a transition at $2n_0$ is equivalent to a transition density of $3 - 4n_0$ for symmetric matter. In particular, it is well known that isospin-symmetric systems are bound in atomic nuclei whereas there are no bound systems of only neutrons known in nature. This is due to the effect of the asymmetry energy in nuclear matter which stiffens isospin-asymmetric systems as compared to the symmetric case. The consequence that the onset density for deconfinement is lowered with increasing asymmetry has been discussed in the literature before. For example, the effect is illustrated in Fig. 1 of [81] for the example of collisions of asymmetric nuclei (Au+Au), where a lowering of the onset density to $4n_0$ from $\sim 6n_0$ in the symmetric case was obtained. For beta-equilibrated matter in neutron stars the lowering is still more pronounced. In Fig. 13 of [82], the phase transition onset density of $2.5n_0$ has been obtained for a model of beta-equilibrated matter with a Maxwell construction, while effects of inhomogeneities may lower the onset density further. For the

extreme case of a Glendenning construction [83] (neglecting surface tension), the lowering of the phase transition density has been shown in Fig. 1 of [84]. A possible onset density of $2n_0$ in neutron star matter is realistic and does not contradict the phenomenology of heavy-ion collisions, where in almost symmetric nuclear matter the transition is not expected at these low densities.

All models have been supplemented with the low-density EOSs of crustal matter according to [85, 86]. The pressure vs energy density for each EOS in our sample is plotted in Fig. 1.

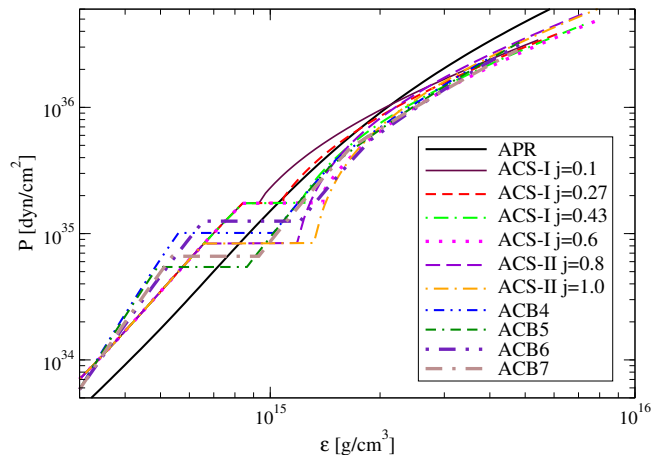


FIG. 1. Pressure vs energy density for the equations of state with first-order phase transitions we consider in this work.

III. METHODS

To test whether the Set I and Set II EOSs satisfy the TD constraints set by GW170817, we adopt tabulated versions of the EOSs we developed and compute sequences of nonrotating HSs for each EOS. For every member of the sequence, we compute the dimensionless TD parameter $\Lambda = \lambda^{(\text{tid})}/M^5$ (in the small tidal deformation approximation), where $\lambda^{(\text{tid})}$ is the stellar TD parameter and M the stellar gravitational mass. For more details on the calculation of Λ , see [61, 87–89].

To investigate the I-Love-Q relations for both slowly and rapidly rotating HSs we compute the dimensionless moment of inertia $\bar{I} = I/M^3$ (with I being the stellar moment of inertia), Λ , and the dimensionless quadrupole moment $\bar{Q} = -Q/(M^3\chi^2)$. Here, Q is the spin-induced quadrupole moment (see [90, 91]), and $\chi = J/M^2$, with J the total angular momentum. The calculation of these quantities in the slow-rotation approximation is performed as in [61] following the Hartle-Thorne formalism [92, 93]. For rapidly rotating stars, we compute \bar{I} and \bar{Q} for sequences of self-consistent, rotating stellar equilibrium configurations that we build with the code of [94–97]. More specifically, \bar{Q} is calculated through the asymptotic structure of the spacetime as described

in [98]. We checked the consistency of the two different codes in the slow-rotation regime.

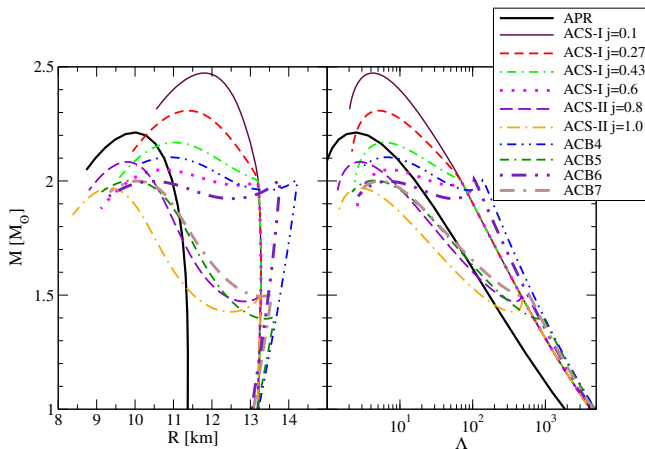


FIG. 2. Left: Mass-radius relation for nonrotating HSs. Observe that some EOSs admit a stable third family branch (separate from the stable NS branch). Right: Mass-TD relation for nonrotating stars with the same EOSs. The APR EOS is also shown for comparison.

IV. RESULTS

The $M - R$ (here R is the stellar areal radius) relations for nonrotating HSs with the Set I and Set II EOSs are shown in the left panel of Fig. 2. For comparison we also show the APR EOS [99]. The $M - R$ plot demonstrates that for the ACS-I $j = 0.43$, ACS-I $j = 0.6$, ACS-II and ACB EOSs a third family of hybrid hadron-quark stars emerges. All EOS parametrizations we developed here satisfy the $2M_{\odot}$ bound for the maximum mass. The ACS-I $j = 0.6$, ACB 4 and ACB 6 models give rise to high mass ($\sim 2.0M_{\odot}$) twins, while the ACS-II and ACB 5 and ACB 7 models lead to low-mass ($\sim 1.5M_{\odot}$) HSs.

The right panel of Fig. 2 shows the $M - \Lambda$ relation for the same configurations as in the left panel. Notice that when the third family branch emerges at low masses, $\Lambda(M)$ can no longer be approximated as a linear function as was found in [100]. As a result, the method adopting this approximation to estimate the tidal deformability of a $1.4M_{\odot}$ compact object [101], and which was used in the case of GW170817 [9], excludes the possibility of low-mass HSs in the third family.

In Fig. 3 we plot the TDs Λ_1 vs Λ_2 for binary compact objects with the chirp mass of GW170817, i.e., $\mathcal{M} = 1.188M_{\odot}$. We show curves corresponding to Set I and Set II EOSs, as well as the 50% and 90% credible constraints set by GW170817 with low-spin prior $|\chi| < 0.05$ (in the left panel). We find that the ACS-I and ACS-II, ACB5-7 EOSs are consistent with the 90% credible upper bound set by GW170817, while ACB4 is inconsistent. Notice that different ACS-I EOSs are indistinguishable from each other for $\Lambda \geq 70$ (see the right

panel of Fig. 2). Thus, we only show one curve for ACS-I. An important finding is that while certain hadronic EOSs may not satisfy the GW170817 constraints on the TD, they can become compatible with GW170817 if a first-order phase transition occurs in one of the stars and it is a HS in the 3rd family branch. This is exemplified by our ACB4 and 5 models which are matched to the same hadronic baseline EOS. In particular, the hadronic (solid) parts of the $\Lambda_1 - \Lambda_2$ curve that corresponds to them are excluded by GW170817 at 90% confidence, but the HS-NS (dashed-dotted) ACB5 curve satisfies the GW170817 90% confidence constraints on the TD. Apart from ACB5, the ACB7 and ACS-II EOSs satisfy the constraints set by GW170817 when having one star in the normal hadronic branch and the other one in the third family (the dot-dashed branch of a given color curve). Therefore, *GW170817 is consistent with the coalescence of a binary HS-NS.*

One finds similar results for the high-spin prior GW170817 TD constraints within the range $\Lambda_2 < 3000$ (see right panel in Fig. 3), but ACB4 is only marginally inconsistent with the 90% credible constraints. However, since the mass of the primary star can be as large as $2.26M_{\odot}$, the HS/NS scenario may be consistent with GW170817 even for equations of state with the transition happening in the high mass regime. Investigating this possibility further is beyond the scope of this paper as the bound in the $\Lambda_1 - \Lambda_2$ plane for $\Lambda_2 > 3000$ is not provided in [9].

In Fig. 4 we show the I-Love-Q relations for slowly rotating and rapidly rotating stars constructed with the Set I and Set II EOSs. Following [102] we generated χ -constant sequences for rapidly rotating stars. Notice that the relations for slowly rotating stars remain universal and agree with those reported for neutron stars and quark stars in [62]. Notice also that the I-Q relations for rapidly rotating stars remain universal for a fixed χ , in agreement with [102, 103]. The deviations from universality with the hybrid hadron-quark EOSs considered here are slightly larger than those in [62], especially for high mass (small Λ or \bar{Q}) stars. Nevertheless, the relations remain universal within $\sim 3\%$ for both slowly and rapidly rotating stars. Thus, our results extend the previously discovered universal I-Love-Q relations for compact stars into the third family.

V. DISCUSSION

We have constructed hybrid hadron-quark EOSs that: i) give rise to a third family of compact objects, ii) are consistent with the existence of $2M_{\odot}$ pulsars, and iii) result in low-mass twins ($\sim 1.5M_{\odot}$). Using our new model EOSs we computed the TD of sequences of relativistic stars. In contrast to realistic neutron star EOSs, where the dimensionless tidal deformability can be approximated as a linear function of the gravitational mass in the vicinity of $1.4M_{\odot}$, in the case of hybrid hadron-

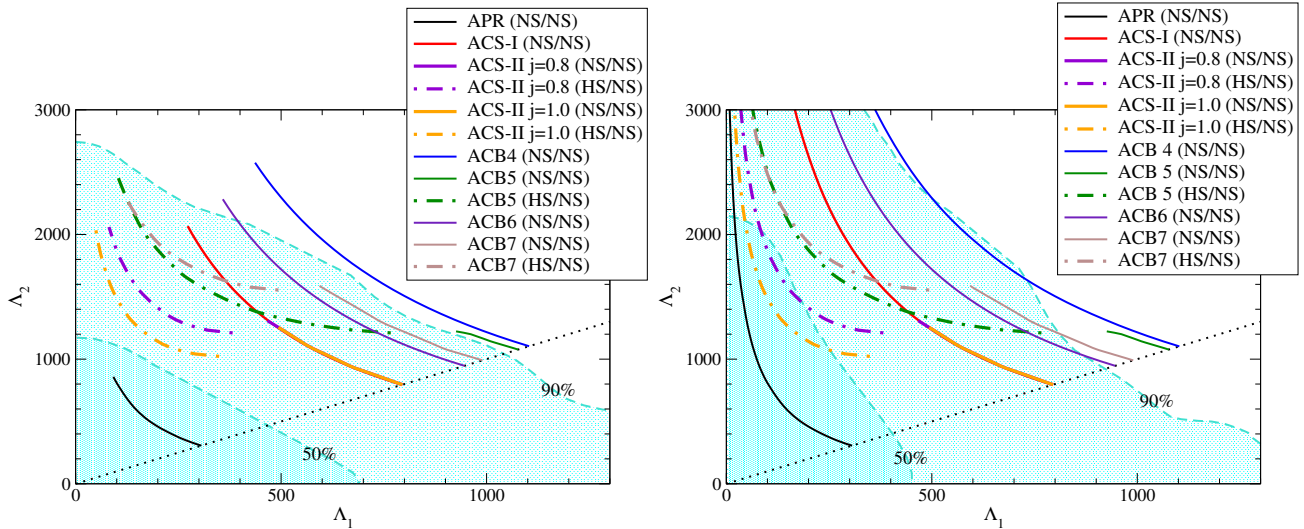


FIG. 3. TDs of compact objects in GW170817 with chirp mass $\mathcal{M} = 1.188M_{\odot}$ for the ACS-I (which are indistinguishable from each other for $\Lambda \geq 70$), ACS-II and ACB EOSs. Solid curves correspond to both stars being in the NS branch while dashed-dotted curves correspond to one of the stars being in the third family (namely HSs). Note that the gap between the solid and dashed-dotted component of a given color curve arises because the HS member in the binary is unstable. Only the plot above the black dotted line ($\Lambda_1 = \Lambda_2$) is relevant. The dark and light cyan shaded areas correspond to the parameter region within the 50% and 90% credible upper bound set by GW170817 with prior $|\chi| < 0.05$ (left panel) and $|\chi| < 0.89$ (right panel). The solid black curve corresponds to the APR EOS.

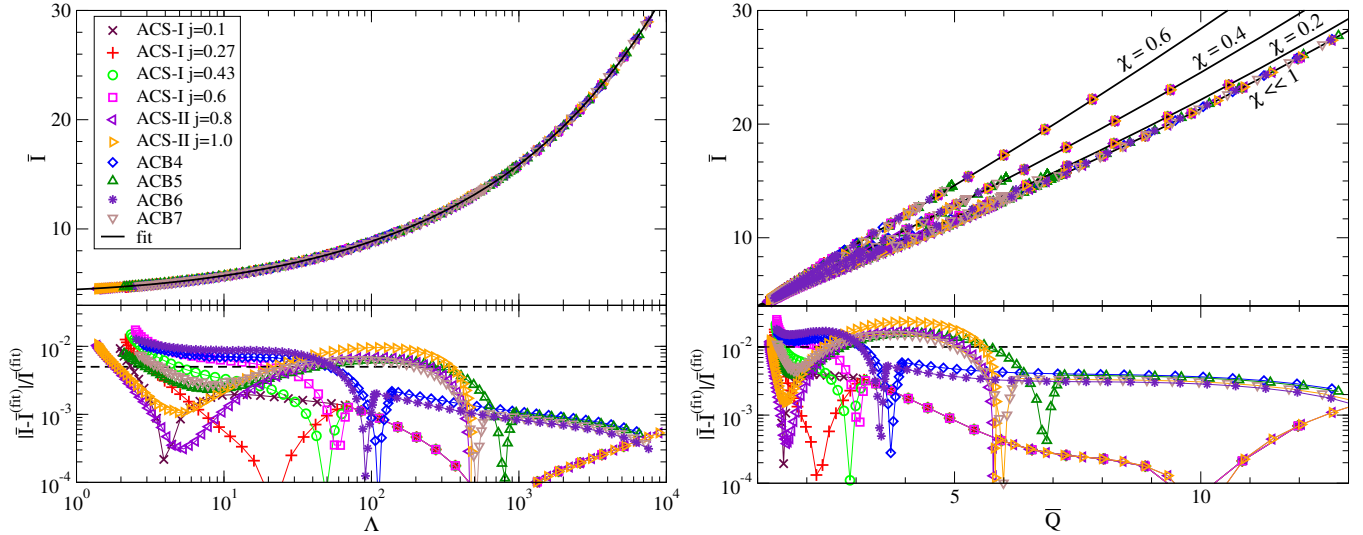


FIG. 4. Left: I-Love relations for slowly rotating stars together with the analytic fit of [62]. Right: I-Q relation for slowly and rapidly rotating stars with various dimensionless spin parameters χ together with the analytic fit in [102]. In both panels $|\bar{I} - \bar{I}^{(\text{fit})}| / \bar{I}^{(\text{fit})}$ is the fractional difference between the numerical results and the corresponding analytic fits. The horizontal dashed lines in the $|\bar{I} - \bar{I}^{(\text{fit})}| / \bar{I}^{(\text{fit})}$ plots indicate the maximum fractional difference between the numerical results and the fits reported in [62].

quark EOSs with low-mass twins this is no longer true. As a result, using this approximation to estimate the tidal deformability of a $1.4M_{\odot}$ compact objects should be avoided because it excludes the possibility of testing for HSs. All EOSs in our sample, except for one, are consistent with the GW170817 90% confidence TD bounds. We discover that while a sufficiently stiff hadronic base-

line EOS may be inconsistent with GW170817, a hadron-quark phase transition in the compact object interior can soften the EOS to make it compatible with GW170817. Importantly, we find that GW170817 is entirely consistent with coalescence of a binary hybrid hadron-quark – neutron star.

Furthermore, we computed the I-Q relations [104]

for rotating relativistic stars adopting our new hybrid hadron-quark EOSs, and discover that despite the sharp first-order phase transition at the hadron-quark interface in the interior of these stars, the hybrid star I-Q relations agree with the I-Q relations of slowly and rapidly rotating realistic neutron stars and quark stars to better than $\sim 3\%$. Therefore, the I-Love-Q relations can be adopted to either perform equation-of-state independent tests of general relativity or to break degeneracies in parameter estimation from GWs even when HSs in the third family are present.

Future GW observations will help understand the properties of hybrid stars and resolve the current controversy about the nature of the hadron-to-quark matter transition at zero temperature: is it a first-order transition with large jump in energy density or is it a smooth crossover? At this time, it seems that the only possible way to constrain the nature of binary compact objects through GWs, and hence to resolve the aforementioned controversy requires GW detectors that are sensitive in the high frequency regime, where tidal effects are strong and can lead to measurable deviations between the GWs generated by binary NS-NS and binary HS-NS. To address this point theoretically it is necessary to perform binary HS-NS simulations in full general relativity and compare them to NS-NS simulations. Our work sets the foundations for performing such an analysis by constructing the equations of state that respect all currently known constraints.

Another way to probe the aforementioned controversy

is to combine GW and electromagnetic observations of compact objects. For example, if the presently ongoing NICER [105] measures the radius of the $1.44M_{\odot} \pm 0.07$ pulsar J0437-4715 to not be less than 14 km with an uncertainty of less than 500 m, then soft hadronic EOSs would be incompatible, and the stiff hadronic baseline of the set of EOSs discussed here would be favored. However, according to [48], a hadronic EOS with $R_{1.4} > 13.4$ km is inconsistent with GW170817; thus, the HS-NS scenario for GW170817 would be a most likely explanation, implying an EOS with a stiff hadronic part and a strong phase transition.

ACKNOWLEDGMENTS

D.E.A.-C. is grateful for support by the ExtreMe Matter Institute EMMI at the GSI Helmholtzzentrum für Schwerionenphysik Darmstadt, Germany, as well as to the Heisenberg-Landau and Bogoliubov-Infeld programs for collaboration between JINR Dubna and Institutions in Germany and Poland, respectively. D.B. is supported by the Russian Science Foundation under Contract No. 17-12-01427. D.E.A.-C., D.B. and A.S. acknowledge partial support by the COST Action MP1304 (NewCompStar) for networking activities. A.S. is supported by the Deutsche Forschungsgemeinschaft (Grant No. SE 1836/3-2). K.Y. would like to acknowledge networking support by the COST Action GWverse CA16104.

-
- [1] B. P. Abbott *et al.* (LIGO Scientific Collaboration and Virgo Collaboration), *Phys. Rev. Lett.* **116**, 061102 (2016).
 - [2] B. P. Abbott *et al.* (Virgo, LIGO Scientific), *Phys. Rev. Lett.* **116**, 241103 (2016).
 - [3] B. P. Abbott *et al.* (VIRGO, LIGO Scientific), *Phys. Rev. Lett.* **118**, 221101 (2017).
 - [4] B. P. Abbott *et al.* (Virgo, LIGO Scientific), *Phys. Rev. Lett.* **119**, 141101 (2017).
 - [5] B. P. Abbott *et al.* (Virgo, LIGO Scientific), *Astrophys. J.* **851**, L35 (2017).
 - [6] B. P. Abbott *et al.* (Virgo, LIGO Scientific), *Astrophys. J.* **818**, L22 (2016).
 - [7] B. P. Abbott *et al.* (Virgo, LIGO Scientific), *Phys. Rev. Lett.* **116**, 221101 (2016).
 - [8] N. Yunes, K. Yagi, and F. Pretorius, *Phys. Rev.* **D94**, 084002 (2016).
 - [9] B. Abbott *et al.* (Virgo, LIGO Scientific), *Phys. Rev. Lett.* **119**, 161101 (2017).
 - [10] B. P. Abbott *et al.*, *Astrophys. J. Lett.* **848**, L13 (2017).
 - [11] B. P. Abbott *et al.*, *Astrophys. J. Lett.* **848**, L12 (2017).
 - [12] B. P. Abbott *et al.* (Virgo, LIGO Scientific), *Astrophys. J.* **850**, L39 (2017).
 - [13] S. J. Smartt *et al.*, *Nature* **551**, 75 (2017).
 - [14] P. S. Cowperthwaite *et al.*, *Astrophys. J.* **848**, L17 (2017).
 - [15] M. Nicholl *et al.*, *Astrophys. J.* **848**, L18 (2017).
 - [16] R. Chornock *et al.*, *Astrophys. J.* **848**, L19 (2017).
 - [17] R. Margutti *et al.*, *Astrophys. J.* **848**, L20 (2017).
 - [18] D. A. Coulter, R. J. Foley, C. D. Kilpatrick, M. R. Drout, A. L. Piro, B. J. Shappee, M. R. Siebert, J. D. Simon, N. Ulloa, D. Kasen, B. F. Madore, A. Murguía-Berthier, Y.-C. Pan, J. X. Prochaska, E. Ramirez-Ruiz, A. Rest, and C. Rojas-Bravo, *Science*.
 - [19] B. P. Abbott *et al.* (LIGO Scientific, VINROUGE, Las Cumbres Observatory, DES, DLT40, Virgo, 1M2H, Dark Energy Camera GW-E, MASTER), *Nature* **551**, 85 (2017).
 - [20] B. D. Metzger, (2017), [arXiv:1710.05931 \[astro-ph.HE\]](https://arxiv.org/abs/1710.05931).
 - [21] B. Paczynski, *Astrophys. J. Lett.* **308**, L43 (1986).
 - [22] D. Eichler, M. Livio, T. Piran, and D. N. Schramm, *Nature* **340**, 126 (1989).
 - [23] R. Narayan, B. Paczynski, and T. Piran, *Astrophys. J. Lett.* **395**, L83 (1992).
 - [24] V. Paschalidis, M. Ruiz, and S. L. Shapiro, *Astrophys. J. Lett.* **806**, L14 (2015).
 - [25] M. Ruiz, R. N. Lang, V. Paschalidis, and S. L. Shapiro, *Astrophys. J.* **824**, L6 (2016).
 - [26] V. Paschalidis, *Class. Quant. Grav.* **34**, 084002 (2017).
 - [27] L. Baiotti and L. Rezzolla, *Rept. Prog. Phys.* **80**, 096901 (2017).
 - [28] B. P. Abbott *et al.* (Virgo, LIGO Scientific), *Astrophys. J.* **850**, L40 (2017).

- [29] B. P. Abbott *et al.* (Virgo, LIGO Scientific), *Phys. Rev. Lett.* **120**, 091101 (2018).
- [30] J. Sakstein and B. Jain, *Phys. Rev. Lett.* **119**, 251303 (2017).
- [31] S. Jana, G. K. Chakravarty, and S. Mohanty, (2017), [arXiv:1711.04137 \[gr-qc\]](#).
- [32] S. Nojiri and S. D. Odintsov, *Phys. Lett.* **B779**, 425 (2018).
- [33] M. A. Green, J. W. Moffat, and V. T. Toth, *Phys. Lett.* **B780**, 300 (2018), [arXiv:1710.11177 \[gr-qc\]](#).
- [34] T. Baker, E. Bellini, P. G. Ferreira, M. Lagos, J. Noller, and I. Sawicki, *Phys. Rev. Lett.* **119**, 251301 (2017).
- [35] J. M. Ezquiaga and M. Zumalacregui, *Phys. Rev. Lett.* **119**, 251304 (2017).
- [36] P. Creminelli and F. Vernizzi, *Phys. Rev. Lett.* **119**, 251302 (2017).
- [37] L. Heisenberg and S. Tsujikawa, *JCAP* **1801**, 044 (2018).
- [38] L. Lombriser and A. Taylor, *JCAP* **1603**, 031 (2016).
- [39] L. Lombriser and N. A. Lima, *Phys. Lett.* **B765**, 382 (2017).
- [40] B. F. Schutz, *Nature* **323**, 310 (1986).
- [41] P. B. Demorest, T. Pennucci, S. M. Ransom, M. S. E. Roberts, and J. W. T. Hessels, *Nature* **467**, 1081 (2010).
- [42] J. Antoniadis *et al.*, *Science* **340**, 6131 (2013), [arXiv:1304.6875 \[astro-ph.HE\]](#).
- [43] E. Fonseca *et al.*, *Astrophys. J.* **832**, 167 (2016).
- [44] Z. Arzoumanian *et al.*, *Astrophys. J. Suppl.* **235**, 37 (2018), [arXiv:1801.01837 \[astro-ph.HE\]](#).
- [45] S. Benić, D. Blaschke, D. E. Alvarez-Castillo, T. Fischer, and S. Typel, *Astron. Astrophys.* **577**, A40 (2015).
- [46] D. E. Alvarez-Castillo and D. B. Blaschke, *Phys. Rev.* **C96**, 045809 (2017).
- [47] M. Alford and A. Sedrakian, *Phys. Rev. Lett.* **119**, 161104 (2017).
- [48] E. Annala, T. Gorda, A. Kurkela, and A. Vuorinen, (2017), [arXiv:1711.02644 \[astro-ph.HE\]](#).
- [49] A. Bauswein, O. Just, H.-T. Janka, and N. Stergioulas, *Astrophys. J.* **850**, L34 (2017).
- [50] M. Ruiz, S. L. Shapiro, and A. Tsokaros, *Phys. Rev.* **D97**, 021501 (2018).
- [51] D. Radice, A. Perego, F. Zappa, and S. Bernuzzi, *Astrophys. J.* **852**, L29 (2018).
- [52] L. Rezzolla, E. R. Most, and L. R. Weih, *Astrophys. J.* **852**, L25 (2018).
- [53] M. Shibata, S. Fujibayashi, K. Hotokezaka, K. Kiuchi, K. Kyutoku, Y. Sekiguchi, and M. Tanaka, *Phys. Rev.* **D96**, 123012 (2017).
- [54] B. Margalit and B. D. Metzger, *Astrophys. J.* **850**, L19 (2017).
- [55] E. Zhou, X. Zhou, and A. Li, (2017), [arXiv:1711.04312 \[astro-ph.HE\]](#).
- [56] U. H. Gerlach, *Phys. Rev.* **172**, 1325 (1968).
- [57] B. Kämpfer, *J. of Phys. A: Math. Gen.* **14**, L471 (1981).
- [58] K. Schertler, C. Greiner, J. Schaffner-Bielich, and M. H. Thoma, *Nucl. Phys. A* **677**, 463 (2000).
- [59] N. K. Glendenning and C. Kettner, *Astron. Astrophys.* **353**, L9 (2000).
- [60] K. Yagi and N. Yunes, *Science* **341**, 365 (2013).
- [61] K. Yagi and N. Yunes, *Phys. Rev.* **D88**, 023009 (2013).
- [62] K. Yagi and N. Yunes, *Phys. Rept.* **681**, 1 (2017).
- [63] V. Paschalidis and N. Stergioulas, *Living Rev. Rel.* **20**, 7 (2017).
- [64] D. D. Doneva and G. Pappas, (2017), [arXiv:1709.08046 \[gr-qc\]](#).
- [65] Note that in [106], which appeared after our work, it is claimed that the I-Love-Q relations do not hold for HSS.
- [66] P. Ring, *J. of Phys.: Conf. Series* **205**, 012010 (2010).
- [67] G. A. Lalazissis, T. Nikšić, D. Vretenar, and P. Ring, *Phys. Rev. C* **71**, 024312 (2005).
- [68] G. Colucci and A. Sedrakian, *Phys. Rev. C* **87**, 055806 (2013).
- [69] K. Hebeler, J. M. Lattimer, C. J. Pethick, and A. Schwenk, *Astrophys. J.* **773**, 11 (2013).
- [70] D. Alvarez-Castillo, A. Ayriyan, S. Benic, D. Blaschke, H. Grigorian, and S. Typel, *Eur. Phys. J.* **A52**, 69 (2016).
- [71] N. K. Glendenning, *Compact Stars: Nuclear Physics, Particle Physics, and General Relativity*, Astronomy and astrophysics library (Springer, 1997).
- [72] F. Weber, *Pulsars as astrophysical laboratories for nuclear and particle physics* (Institute of Physics, Bristol, 1999).
- [73] M. G. Alford, S. Han, and M. Prakash, *Phys. Rev. D* **88**, 083013 (2013).
- [74] Z. F. Seidov, *Sov. Ast.* **15**, 347 (1971).
- [75] J. L. Zdunik and P. Haensel, *Astron. Astrophys.* **551**, A61 (2013).
- [76] L. Bonanno and A. Sedrakian, *Astron. Astrophys.* **539**, A16 (2012).
- [77] N. S. Ayzvazyan, G. Colucci, D. H. Rischke, and A. Sedrakian, *Astron. Astrophys.* **559**, A118 (2013).
- [78] M. A. R. Kaltenborn, N.-U. F. Bastian, and D. B. Blaschke, *Phys. Rev.* **D96**, 056024 (2017).
- [79] J. S. Read, B. D. Lackey, B. J. Owen, and J. L. Friedman, *Phys. Rev. D* **79**, 124032 (2009).
- [80] C. A. Raithel, F. Ozel, and D. Psaltis, *Astrophys. J.* **831**, 44 (2016).
- [81] M. Di Toro, B. Liu, V. Greco, V. Baran, M. Colonna, and S. Plumari, *Phys. Rev.* **C83**, 014911 (2011).
- [82] T. Fischer, N.-U. Bastian, D. Blaschke, M. Cerniak, M. Hempel, T. Klähn, G. Martnez-Pinedo, W. G. Newton, G. Röpke, and S. Typel, *Publ. Astron. Soc. Austral.* **34**, e067 (2017).
- [83] N. K. Glendenning, *Phys. Rev. D* **46**, 1274 (1992).
- [84] I. Sagert, T. Fischer, M. Hempel, G. Pagliara, J. Schaffner-Bielich, A. Mezzacappa, F. K. Thielemann, and M. Liebendörfer, *Phys. Rev. Lett.* **102**, 081101 (2009).
- [85] G. Baym, C. Pethick, and P. Sutherland, *Astrophys. J.* **170**, 299 (1971).
- [86] J. W. Negele and D. Vautherin, *Nucl. Phys. A* **207**, 298 (1973).
- [87] T. Hinderer, *Astrophys. J.* **677**, 1216 (2008).
- [88] T. Damour and A. Nagar, *Phys. Rev.* **D80**, 084035 (2009).
- [89] T. Binnington and E. Poisson, *Phys. Rev.* **D80**, 084018 (2009).
- [90] J. L. Friedman and N. Stergioulas, *Rotating Relativistic Stars*, Cambridge Monographs on Mathematical Physics (Cambridge University Press, 2013).
- [91] G. Pappas and T. A. Apostolatos, *Phys. Rev. Lett.* **108**, 231104 (2012).
- [92] J. B. Hartle, *Astrophys. J.* **150**, 1005 (1967).

- [93] J. B. Hartle and K. S. Thorne, *Astrophys. J.* **153**, 807 (1968).
- [94] G. Cook, S. Shapiro, and S. Teukolsky, *Astrophys. J.* **398**, 203 (1992).
- [95] G. Cook, S. Shapiro, and S. Teukolsky, *Astrophys. J.* **423**, L117 (1994).
- [96] G. Cook, S. Shapiro, and S. Teukolsky, *Astrophys. J.* **424**, 823 (1994).
- [97] G. Cook, S. Shapiro, and S. Teukolsky, *Astrophys. J.* **422**, 227 (1994).
- [98] D. D. Doneva, S. S. Yazadjiev, N. Stergioulas, and K. D. Kokkotas, *Astrophys. J.* **781**, L6 (2013).
- [99] A. Akmal, V. R. Pandharipande, and D. G. Ravenhall, *Phys. Rev. C* **58**, 1804 (1998).
- [100] T. Damour, A. Nagar, and L. Villain, *Phys. Rev. D* **85**, 123007 (2012).
- [101] W. Del Pozzo, T. G. F. Li, M. Agathos, C. Van Den Broeck, and S. Vitale, *Phys. Rev. Lett.* **111**, 071101 (2013).
- [102] S. Chakrabarti, T. Delsate, N. Gürlebeck, and J. Steinhoff, *Phys. Rev. Lett.* **112**, 201102 (2014).
- [103] G. Pappas and T. A. Apostolatos, *Phys. Rev. Lett.* **112**, 121101 (2014).
- [104] We do not compute the I-Love relations for rapidly rotating relativistic stars as the formulation for computing the tidal Love numbers for such stars is currently lacking. Various tidal Love numbers for slowly rotating stars have been computed to leading order in spin in [107], though the spin correction to Λ that we consider here enters first at quadratic order in spin.
- [105] K. C. Gendreau *et al.*, “The neutron star interior composition explorer (nicer): design and development,” (2016).
- [106] D. Bandyopadhyay, S. A. Bhat, P. Char, and D. Chatterjee, *Eur. Phys. J.* **A54**, 26 (2018).
- [107] P. Pani, L. Gualtieri, and V. Ferrari, *Phys. Rev.* **D92**, 124003 (2015).